GM75 model. The vertical wave number spectral estimates have been compensated for aliasing (*11*, pp. 52–53), assuming an asymptotic $\beta^{-2.5}$ dependence consistent with the GM75 model. Because the data are averaged horizontally over scales smaller than the sampling interval, the horizontal spectrum is not aliased. Also plotted in Fig. 1 are normalized one-dimensional spectral estimates drawn from several published sources (*3, 13, 14*), together with the appropriate predictions of the GM75 model. Clearly, our data are consistent with the historical data, and the GM75 model gives a fair representation of the one-dimensional spectra.

Our empirical two-dimensional spectrum is presented in Fig. 2A. Since there are no data relating to the correct asymptotic form of the two-dimensional spectrum, no attempt has been made to compensate for aliasing in the vertical. The presentation is in the form of a contour map. The wave number axes are logarithmic, and the data are represented by computer-generated contours of $\log(N/N_0)F_\zeta(\alpha_1, \beta)$, the units of F being (meters)^2 (cycles per meter)$^{-2}$. Along any curve (contour) $F_\zeta(\alpha_1, \beta)$ is constant, and successive contour levels are separated by 5-db increments in F. Small-scale vacillations in the contours are the result of statistical variability related to the finiteness of our data sample. The spectrum is roughly symmetric about the line $\beta = \alpha_1 N/f$, which corresponds to a (45°) diagonal passing through the point (α_1, β) = (0.2 cycle/km, 0.025 cycle/m).

This behavior is consistent with the results of a scale analysis of the internal wave equation, which indicate that vertical and horizontal dimensions in the internal wave field should scale roughly in the ratio f/N, where f is the local inertial frequency (2 cycles per day times the sine of the latitude). The corresponding GM75 model spectrum is plotted in Fig. 2B, and although the model gives a fair representation of the data for $\beta \lesssim \alpha_1 N/f$, it exhibits a trend of systematic deviation from the data for $\beta \gtrsim \alpha_1 N/f$. This trend is emphasized in Fig. 2C, where we have contoured the logarithm of the ratio of the empirical spectral density to the model spectral density—that is, the difference between A and B of Fig. 2. The effect of aliasing on the measured spectrum should be confined to a narrow band along the top of Fig. 2C, the maximum effect being a 3-db (0.3 unit of log F) rise in the spectrum at $\beta = 0.4$ cycle/m. Taking into account the vertical aliasing, it would appear that the deviation is primarily a function of the ratio α_1/β. Since the frequency–wave number dispersion relation takes the form

$$\omega^2 = f^2(1 + \alpha^2 N^2/\beta^2 f^2)$$

for waves with frequency $\omega \ll N$, this implies that the deviation is primarily a function of frequency, rather than wave number per se. That is, the GM75 model systematically underestimates the measured spectrum as ω tends down to the inertial frequency. Note that this systematic deviation is much less apparent in the integrated or one-dimensional spectra, although a close examination of Fig. 1 indicates that the GM75 model does not precisely predict the data. Unfortunately, conversion of the α_1-β spectra to a frequency spectrum via the dispersion relation greatly amplifies the statistical "noise" in the experimental data since the derivative $\delta F/\delta\alpha_1$ is required in order to estimate $F(\alpha,\beta;\omega(\alpha,\beta))$, so that a meaningful quantitative comparison of our data with historical data from moored sensors is virtually impossible. However, we do note that the nature of the deviation between GM75 and our data appears at least to be consistent with the fact that although simple wave theory (as incorporated in the GM75 model) dictates that inertial period motions produce no sensible vertical displacements, vertical displacements are indeed found to be associated with inertial period motions in the sea (*15*).

T. H. Bell, Jr., J. M. Bergin
J. P. Dugan, Z. C. B. Hamilton
W. D. Morris, B. S. Okawa, E. E. Rudd
Ocean Sciences Division,
Naval Research Laboratory,
Washington, D.C. 20375

References and Notes

1. N. P. Fofonoff and F. Webster, *Philos. Trans. R. Soc. Lond. Ser. A Math. Phys. Sci.* **270**, 349 (1971); W. J. Gould, *ibid.*, p. 437.
2. C. Garrett and W. Munk, *Geophys. Fluid Dyn.* **3**, 225 (1972); *J. Geophys. Res.* **80**, 291 (1975).
3. E. J. Katz, *J. Phys. Oceanogr.* **3**, 448 (1973).
4. S. A. Kitaygorodskiy, Yu. Z. Miropol'skiy, B. N. Filyushkin, *Izv. Akad. Nauk SSSR Phys. Atmos. Okean.* **9**, 272 (1973).
5. For the data analyzed here, the skewness of the probability density function is 0.01 and the kurtosis is 3.73.
6. A. M. Yaglom, *An Introduction to the Theory of Stationary Random Functions*, translated and edited by R. A. Silverman (Prentice-Hall, Englewood Cliffs, N.J., 1962), p. 15.
7. Because of peculiarities of chain construction and towing configuration, there is a systematic variability of ± 0.24 m in thermistor spacing. However, numerical studies indicate that this variability has little effect on our spectral decomposition, and we treat the data as if they were uniformly spaced in the vertical.
8. T. H. Bell, *J. Phys. Oceanogr.* **4**, 669 (1974).
9. Using the frequency–wave number dispersion relation for internal waves, it is readily established that the average internal wave phase speed in the direction of tow for each vertical-horizontal wave number pair resolved by our array is small compared to the tow speed, and we are thereby justified in replacing elapsed time by horizontal distance in our analysis of the data.
10. The total deviation from the vertical of the active portion of the chain considered here was less than the 105-m averaging interval, so that for purposes of analysis the 64 × 32 point data grids represent matrices of uniformly spaced smooth temperatures. See also (*7*).
11. G. M. Jenkins and D. G. Watts, *Spectral Analysis and Its Applications* (Holden-Day, San Francisco, 1968).
12. T. H. Bell, *Geophys. Res. Lett.* **1**, 253 (1974); R. S. McKean and T. E. Ewart, *J. Phys. Oceanogr.* **4**, 191 (1974).
13. A. D. Voorhis and H. T. Perkins, *Deep-Sea Res.* **13**, 641 (1966).
14. N. G. Garnich, Yu. Z. Miropol'skiy, V. I. Prokhorov, K. N. Federov, *Izv. Akad. Nauk SSSR Phys. Atmos. Okean.* **9**, 155 (1973); S. P. Hayes, T. M. Joyce, R. C. Millard, *J. Geophys. Res.* **80**, 314 (1975).
15. C. Rooth and W. Duing, *J. Phys. Oceanogr.* **1**, 12 (1971).

20 February 1975; revised 9 April 1975

Leukocyte Recruitment to Airways by Cigarette Smoke and Particle Phase in Contrast to Cytotoxicity of Vapor

Abstract. *After hamsters had breathed fresh cigarette smoke in a miniature chamber, airways of the lung showed recruitment of polymorphonuclear leukocytes. Exposure to particles alone by removal of the vapor phase with charcoal did not change the leukocyte response. However, exposure to cigarette smoke vapor after removal of particles with Cambridge filters did not recruit leukocytes but produced nuclear and cytoplasmic vacuoles, double nuclei, and exfoliation of cells.*

Cigarette smoking over a long period is associated with cough, sputum production, and chronic bronchitis in many human subjects (*1*). The mechanism of the bronchitis is unclear. Cigarette smoking and exposure to other airborne agents such as cotton dust are additive in producing chronic bronchitis, as found in cotton textile workers (*2*). Exposure to cotton dust recruited polymorphonuclear leukocytes to nasal airways in human subjects (*3*) and in pulmonary airways of rodents (*4*). The link between cotton dust exposure and cigarette smoking suggested that smoking may recruit leukocytes to airways. The immediate effects of cigarette smoking include reduced early phase of particle clearance (*5*), increased closing volume (*6*), increased airway resistance (*7*), and toxic effects on oral leukocytes (*8*). We now report that in hamsters inhaled cigarette smoke recruits polymorphonuclear (PMN) leukocytes to airway lumens from trachea to terminal bronchioles. The particle phase of the smoke has the same effect. However, the vapor phase alone is cytotoxic to epithelial cells, especially the nonciliated ones.

Hamsters were used to study the immediate effects of airborne exposure to unfiltered whole cigarette smoke, vapor phase alone, and particle phase alone. A novel

method for fixation of lungs at inflation volume preserved particles and cells on the luminal surfaces of airways from trachea to terminal bronchioles. Cells were identified and counted with an optical microscope on cross sections of airways, 1 μm thick and stained with methylene blue. Whole cigarette smoke and particles alone recruited large numbers of PMN leukocytes to walls and lumens of all airways (Table 1).

Groups of four Syrian hamsters of both sexes, each weighing approximately 100 g, were exposed for 4 hours in a specially designed chamber consisting of animal holding tubes between input (nose) and exhaust (tail) manifolds. Unfiltered commercial 100-mm cigarettes were smoked by pulling air through the lighted cigarette into the nose manifold for 2 sec/min. Smoke exposure was timed by a clock that operated a solenoid valve to admit air to the nose chamber for 58 sec/min. Air was removed from the exhaust manifold so that smoke-free air was breathed for about 50 sec/min. Cigarette smoke was filtered through two Cambridge filters to remove particles and expose hamsters to vapor. The vapor phase was removed by pulling the smoke through a drying tube filled with coarse, granular, activated charcoal to expose hamsters to vapor-free particles.

Tobacco extracts were prepared by passing sterile distilled water at 50°C through a filter containing blended cigarette tobacco. The solution and fine particles that passed through the filters were lyophilized and weighed. One hundred milligrams of extract in 100 ml of sterile distilled water was nebulized by a Collison nebulizer into the nose manifold of the chamber. Cotton trash extract prepared in the same way as the tobacco extract, sterile 0.9 percent sodium chloride solution, and sterile water controls were exposed in a similar manner.

For simultaneous exposure to bland particles and the vapor phase of cigarette smoke, finely divided carbon (lamp black) was generated continuously into the chamber by a dust generator. It was measured by weighing the filters used to sample the chamber air. Cigarette smoke vapor (which had passed through two Cambridge filters) was admitted for 2 sec/min.

Immediately after or 2, 8, or 20 hours after exposure, animals were killed by intratracheal fixation of the lungs in situ with 3 to 4 ml of osmium tetroxide suspended in fluorocarbon [1.5 g/100 ml (*9*)] for 15 minutes. This fixed the lungs at inflation volume. Lungs that had been fixed and hardened were removed, sliced sagittally, and postfixed in 2 percent glutaraldehyde in cacodylate buffer for an hour. This method maintains leukocytes and particles on airways and prevents their being washed down from airways into alveoli. Sagittal lung sections were embedded in paraffin and sectioned for histological appraisal of entire lungs. From the adjoining sagittal section 7 to 11 airway cross sections were cut into 2- to 3-mm cubes, dehydrated in ethanol, and embedded in Epon 812 (*10*). These blocks were cut at 1 μm and stained with methylene blue and basic fuchsin to identify and count PMN leukocytes, mononuclear macrophages, and epithelial cells at a magnification of × 1000. Leukocytes and epithelial cells were counted and described for cross sections of two or three airways from groups of two to four animals each and expressed as the ratio of PMN leukocytes to epithelial cells (PMN/Epi) (Table 1). Thereafter, selected areas of blocks were trimmed, sectioned, stained, and examined and photographed with a Philips 300 electron microscope.

Whole (unfiltered) cigarette smoke recruited PMN leukocytes to airways. Progressively more cells appeared at 6 and 12

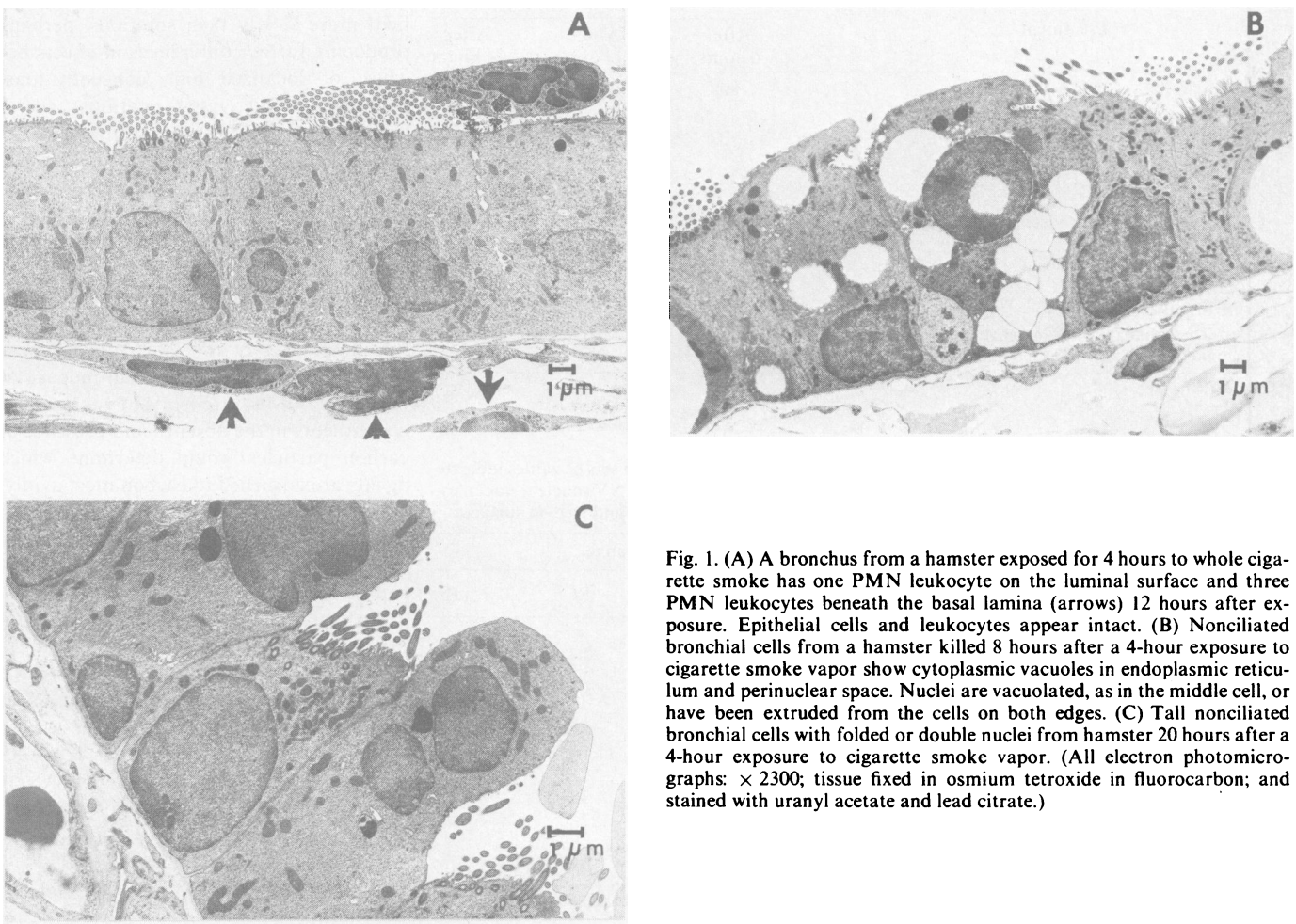

Fig. 1. (A) A bronchus from a hamster exposed for 4 hours to whole cigarette smoke has one PMN leukocyte on the luminal surface and three PMN leukocytes beneath the basal lamina (arrows) 12 hours after exposure. Epithelial cells and leukocytes appear intact. (B) Nonciliated bronchial cells from a hamster killed 8 hours after a 4-hour exposure to cigarette smoke vapor show cytoplasmic vacuoles in endoplasmic reticulum and perinuclear space. Nuclei are vacuolated, as in the middle cell, or have been extruded from the cells on both edges. (C) Tall nonciliated bronchial cells with folded or double nuclei from hamster 20 hours after a 4-hour exposure to cigarette smoke vapor. (All electron photomicrographs: × 2300; tissue fixed in osmium tetroxide in fluorocarbon; and stained with uranyl acetate and lead citrate.)

hours, and the peak effect of 21 to 34 PMN's per 100 epithelial cells was at 24 hours (Table 1; Fig. 1A). Exposure to aerosols of the tobacco extract recruited PMN cells more quickly, with equal numbers at 6 and 12 hours (33 and 32 PMN's per 100 epithelial cells) but with a substantial decrease (6 PMN's per 100 epithelial cells) at 24 hours. The time course of this exposure resembled that of exposure to cotton trash extract, although the cotton trash extract produced a higher peak at 6 hours. A control aerosol of 0.9 percent sodium chloride solution recruited no cells.

Cigarette smoke that had passed through two Cambridge filters to remove particles did not recruit any PMN leukocytes. However, within 24 hours epithelial cell toxicity was manifested by cytoplasmic and perinuclear vacuoles, nuclear vacuoles, loss of cilia, exfoliation of cells, apparent penetration through basal lamina, and double nuclei (Fig. 1, B and C). At 6 hours, cytoplasmic vacuoles were found in 28 percent of nonciliated airway cells, nuclear vacuoles in 6 percent, and 3.8 percent appeared stratified (Table 2). By 12 hours 37 percent had cytoplasmic vacuoles, but 4.8 percent had double nuclei, 8.5 percent had extruded nuclei, and 10 percent had exfoliated. Ciliated cells showed no morphological changes. The difference between 12 and 24 hours was in the thinness of the remaining epithelial cell layer reflecting more cells exfoliated, in more cells with double nuclei, and cells extending beneath the normal basal lamina. These changes together with piling up of cells in small bronchi suggested cell death, then hyperplasia. In contrast, hamsters exposed only to air in the chambers showed neither PMN leukocytes nor cytotoxic changes (Table 2).

Airways of hamsters exposed to bland carbon particles at three high levels (126, 1032, and 1600 mg/m^3) in the air showed no cytotoxic changes and no recruitment of PMN leukocytes. However, when carbon at an intermediate dose (283 mg/m^3) was combined with vapor from cigarette smoke drawn through Cambridge filters, there was PMN leukocyte recruitment of 6.1 at 6 hours, 6.6 at 12, and 31 at 24 hours. Thus it appeared that the vapor phase of cigarette smoke, which was highly toxic by itself, when adsorbed onto carbon was not toxic but recruited PMN leukocytes.

A single exposure to whole cigarette smoke produced the change previously shown to occur from cotton textile plant trash and aerosols of cotton trash (*4*), but the peak effect was delayed to at least 24 hours rather than occurring at 6 hours. However, aerosol exposure to extracts of cigarette tobacco produced the same time course with peak effect at 6 hours. Cigarette smoke particles were responsible for PMN leukocyte recruitment, but when vapor was given simultaneously with carbon particles the effect produced was that of smoke particles.

The cytotoxic effects from exposure to smoke vapor (particles removed) were unexpected. One or more agents in the vapor is cytotoxic. The suggestion that particles play a key role in different effects is supported by the provocative observations from the experiment in which carbon, a particle demonstrated not to recruit leukocytes alone even at extremely high concentrations, did recruit them when vapor, presumably, provided active chemicals to be adsorbed. It also appears that chemicals adsorbed on particles are handled (detoxified) more slowly than solutions, perhaps producing further differences in effects because of localized high concentrations. Cigarette smoke vapor contains several agents that may be responsible for cytotoxicity. These include formaldehyde, hydrogen cyanide, nitrogen dioxide, ammonia, acetaldehyde, acrolein, acetone, and methylethyl ketone (*11*). Of these only nitrogen dioxide has been shown to be cytotoxic and produce nuclear pyknosis and exfoliation of cells (*12*). Formaldehyde is the most toxic of the aldehydes as measured by ciliostasis on tracheal mucosa of rabbits (*13*). Measurements of vapor phase constituents in the absence and presence of carbon particles would determine which agents are adsorbed to carbon most avidly. A series of experimental exposures of single agents and carbon should clarify which are responsible for recruiting leukocytes.

Perhaps the effects shown in these brief experiments may be useful in understanding the pathogenesis of chronic bronchitis in human subjects who smoke cigarettes repeatedly for long periods.

Table 1. Effects of cigarette smoke, particles, vapor, and vapor plus carbon particles on leukocyte recruitment and airway cells. Two sets of values indicate that two experiments were performed. PMN/Epi is the ratio of PMN leukocytes to epithelial cells.

Treatment	(PMN/Epi) × 100		
	After 6 hours	After 12 hours	After 24 hours
Cigarette smoke	8.4	14.7	34.0
		13.7	20.8
Aerosols			
Cigarette tobacco extract (1 mg/ml)	33	32	6
Cotton trash extract (1 mg/ml)	81	33	4
Control saline aerosol	0	0	0
Cigarette smoke with charcoal filter (particles)	7	13	10
	8	7	8
Cigarette smoke with two Cambridge filters (vapor)*	0	0	0
	0	0	0
Controls (air in chamber)	0	0	0
Cigarette smoke (vapor) and carbon (283 mg/m^3)	6.1	6.6	31
Carbon control (126, 1032, and 1600 mg/m^3)	0	0	0

*Cytotoxic changes.

Table 2. Cytotoxic effects of vapor (Cambridge-filtered cigarette smoke). Two sets of values indicate that two experiments were performed. Abbreviations: CV, cellular vacuoles; NV, nuclear vacuoles; NE, nuclei extruded; DN, double nuclei; St, stratified cells; Ex, cell exfoliated and free on surface.

Nonciliated cells (% of total)	Percentage of nonciliated cells with specific change					
	CV	NV	NE	DN	St	Ex
			After 6 hours			
33	28	4.8	0	2.0	4.4	0
24	27	7.8	0.4	1.6	3.3	3.7
			After 12 hours			
31	28.6	7.9	14.0	4.0	3.6	6.7
17	44.8	4.8	3.0	5.6	3.4	13.4
			After 24 hours			
37	15.2	3.6	3.6	8	3.6	3.0*
67	0.8	1.8	0.8	3.1	2.3	0.5*
			Control†			
38	0.1	0.2	0	0.1	0.4	0.2

*Sparse flattened epithelium with areas of denuded basal lamina, cells extended through basal lamina, cilia short or absent. †No differences between 6, 12, and 24 hours.

KAYE H. KILBURN
WAYLAND MCKENZIE
Pulmonary and Environmental Medicine Division, Department of Medicine, University of Missouri–Columbia 65201, and Veterans Administration Hospital, Columbia

References

1. "Smoking and Health," report of the Advisory Committee to the Surgeon General of the Public Health Service [PHS Publ. No. 1103 (1964), p. 280]; O. J. Balchum, J. S. Felton, J. N. Jamison, R. S. Gaines, D. R. Clarke, T. Owan, *Am. Rev. Respir. Dis.* **86**, 675 (1962); C. M. Fletcher and C. M. Tinkler, *Br. Med. J.* **1**, 1491 (1961).
2. J. A. Merchant *et al.*, *J. Occup. Med.* **15**, 212 (1973).
3. J. A. Merchant, G. M. Halprin, A. R. Hudson, K. H. Kilburn, W. N. McKenzie, D. J. Hurst, P. Bermanzohn, *Arch. Environ. Health* **30**, 222 (1975).
4. K. H. Kilburn, W. S. Lynn, L. L. Tres, W. N. McKenzie, *Lab. Invest.* **28**, 55 (1973).
5. R. V. Lourenco, M. F. Klimek, C. J. Borowski, *J. Clin. Invest.* **50**, 1411 (1971).
6. A. S. Buist and B. B. Ross, *Am. Rev. Respir. Dis.* **108**, 1078 (1973).
7. J. A. Nadel and J. H. Comroe, *J. Appl. Physiol.* **16**, 713 (1961).
8. B. Eichel and H. A. Shahrik, *Science* **166**, 1424 (1969).
9. Fluorocarbon (FC-80) from 3M Company, Minneapolis, Minn.
10. J. H. Luft, *J. Biophys. Biochem. Cytol.* **9**, 409 (1961).
11. R. L. Stedman, *Chem. Rev.* **68**, 153 (1968).
12. R. J. Stephens, G. Freeman, M. J. Evans, *Arch. Environ. Health* **24**, 160 (1972).
13. T. Dalhamn and A. Rosenberg, *Arch. Otolaryngol.* **93**, 496 (1971).

28 February 1975; revised 11 April 1975

High-Resolution Scanning Electron Microscopy of Bacteriophages 3C and T4

Abstract. *An account is presented of the design and operation of a new scanning electron microscope, and its first application to the study of biological samples. Bacteriophages were chosen because much of their ultrastructure is beyond the resolution of the conventional scanning electron microscope. The new instrument permits examination of bulk samples with a resolution that exceeds, by at least a factor of 2.5, the resolution obtained in the best secondary electron scanning electron microscopes using high brightness guns, and exceeds by an order of magnitude the resolution of standard scanning electron microscopes using tungsten filament guns. It also permits examination of biological samples in scanning transmission mode at resolutions similar to conventional transmission electron microscopes.*

Although the conventional transmission electron microscope (TEM) and scanning electron microscope (SEM) have enabled the biologist to examine tissues, cells, and minute subcellular structures with great clarity, it is now possible with a single high-resolution SEM to obtain resolution comparable to that of the TEM while operating in the scanning transmission mode (STEM), and resolution an order of magnitude better than that of the standard tungsten filament SEM when examining the surface of bulk samples. The surface resolution is also close to that obtained when the TEM is used to examine biological samples. This report presents surface and transmission micrographs obtained in this instrument, a machine which has its origin in several distinctive modifications in electron microscope design, but which has never previously been used for gathering information from bulk samples of biological materials.

Earlier work with this instrument (*1*) demonstrated that with a lanthanum hexaboride (LaB_6) cathode electron gun and a final lens of short focal length it was possible to produce a beam diameter of 5 Å. Beam diameters of this size had already been obtained with field emission cathodes (*2*); however, field emission cathodes require a vacuum level of better than 1×10^{-9} torr, which is obtained only at the expense of increased complexity, cost, and inconvenience of use. The LaB_6 cathode can be operated in any well-maintained conventional vacuum system ($< 10^{-5}$ torr) using elastomer O-rings, and oil diffusion pumps, as on the majority of commercial electron microscopes.

Initial evaluation of this microscope was by STEM. Subsequently, using a concept proposed by Wells (*3*), a new method for examining bulk samples was found. At that time it had been thought that to form a high-resolution surface image of a bulk sample, it was necessary to collect low-energy secondary electrons from the point of impact of the beam. In order to do this efficiently the sample was always placed outside the magnetic field of the final lens. This necessitated the use of a relatively long focal length final lens with higher aberrations (C_s = 1.8 cm, C_c = 1 cm) than are encountered in the type of short focal length lens (C_s = 0.06 cm, C_c = 0.07 cm) (*4*) used in this microscope. By the new method a bulk sample is placed in the high field region of the lens, and the image formed by collecting primary beam electrons which have been scattered from the sample surface. Wells (*5*) has called this type of image the low-loss image because most of the electrons collected have lost little energy in the sample (< 1000 ev).

Low-loss SEM images obtained in this way provide detailed surface information at a resolution formerly reserved for TEM. At the same time, the images can be easily interpreted in three dimensions as in the conventional long focal length SEM images. Specimen size and low magnification operation are restricted compared to the standard SEM, because the sample is placed in the small lens gap, but this has not proved a significant problem for the examination of small biological samples. In this work we have been able to use the surface mode to observe the morphology of bacteriophages directly, without many of the interpretational problems inherent in transmission electron microscopy. In each case the bacteriophages were also examined in the STEM mode in order to compare our data with previously reported literature in this field.

High-quality secondary images formed with the use of a short focal length final lens SEM have also recently been reported by Kondo and Hasegawa (*6*). Their results, while showing improvement over standard secondary electron images, do not possess the clarity at high magnification that ours possess. It is unclear whether this is due to the improved electron optical performance obtained with the LaB_6 cathode, or is due to the use of high-energy scattered electrons rather than secondaries.

The final lens of the microscope is of the symmetrical condenser-objective type with bores 3 mm in diameter, and a 3-mm gap. For low-loss SEM, the samples are placed in the center of the pole-piece gap. In this position the lens focal length is 1 mm, the spherical aberration coefficient is 0.06 cm, and the chromatic aberration coefficient is 0.07 cm. A beam half angle of 1.4×10^{-2} radian is employed, giving an estimated beam diameter (containing 80 percent of the beam current) of 10 Å for a current of 2×10^{-11} ampere. The gun brightness has been measured to be 9×10^6 amp/cm^2 steradian at the accelerating potential (45 kev) used for this work. The beam diameter as estimated from edge definition in the SEM micrographs is close to, or below, the calculated 10 Å. The electron detector for the low-loss surface mode is a quartz light pipe, 1 cm in diameter, coated with scintillator and a thin layer of aluminum. It is placed approximately 14 cm below the lens gap. A diagram of the detector configuration has already been published (*3*). With the samples examined here, the current reaching the detector varied between 5×10^{-13} amp and 1.5×10^{-12} amp for an incident current to the sample of 2×10^{-11} amp.

For operating in the bright-field STEM mode, an aperture was placed above the scintillator detector. The aperture subtended a half angle of 5×10^{-3} radian at the sample. The beam current for STEM was about 2×10^{-12} amp and the beam diameter was 5 Å.

Log phase *Staphylococcus aureus* (strain 3C), grown on nutrient agar, was inoculated with 3C phage and incubated at 30°C. Samples were taken at 1-, 2-, and 5-hour intervals after inoculation and were

Leukocyte recruitment to airways by cigarette smoke and particle phase in contrast to cytotoxicity of vapor

KH Kilburn and W McKenzie

Science **189** (4203), 634-637.
DOI: 10.1126/science.1162344